Two Renormalization Approaches for the Dyson-Schwinger Equations in the Infrared*

SHI Yuan-Mei[1] PING Jia-Lun[1,2;1)] HE Han-Xin[3]

1 (Department of Physics and Institute of Theoretical Physics, Nanjing Normal University, Nanjing 210097, China)
2 (School of Physics and Microelectronics, Shandong University, Jinan 250100, China)
3 (China Institute of Atomic Energy, Beijing 102413, China)

Abstract Two renormalization approaches: the analytic continuation approach and the subtraction approach, are used to obtain the infrared behavior of gluon and ghost propagators in the coupled gluon and ghost Dyson-Schwinger equations, where the three-gluon and gluon-ghost vertices are taken to be bare. The results show that the two renormalization approaches give the same results in the infrared analysis of propagators.

Key words Dyson-Schwinger equation, non-perturbative QCD, infrared behavior, confinement, renormalization approach

1 Introduction

Quantum chromodynamics (QCD) is believed to be the quantum field theory of the strong interactions of quarks and gluons. In contrast to Abelian gauge theories like quantum electrodynamics (QED), the non-Abelian nature of the gauge symmetry of QCD not only induces interactions between quarks and gluons but also among gluons themselves. This last effect is expected to be responsible for the phenomenon of confinement.

Confinement and the dynamical chiral symmetry breaking are the two genuine effects of non-perturbative QCD. Although there is a lot of work devoted to them, it is still far from satisfactory. Recently the Dyson-Schwinger (DS) approach, equations of motion for correlation functions of the fields, has been employed to study the confinement and the dynamical chiral symmetry breaking[1—3]. The DS approach has been proven to be successful in developing a hadron phenomenology which interpolates smoothly between the infrared (non-perturbative) and the ultraviolet (perturbative) regime[1—3]. Certainly a great step forward in understanding QCD would be the detailed knowledge of the basic correlation functions, the propagators. Information on confinement is encoded in these two-point functions. Furthermore the dynamical chiral symmetry breaking can be studied directly in the DS equation (DSE) for the quark propagator, which is the gap equation of QCD. Besides being related to the fundamentals of QCD, the quark and gluon propagators are vital ingredients for phenomenological models describing low and medium energy hadron physics[4]. Bound state calculations based on the Bethe-Salpeter equations for mesons or the Faddeev equations for baryons[5—9], might one day be capable to bridge the gap between the fundamental theory QCD and phenomenology.

In this paper, we will investigate the behavior of gluon and ghost propagators in the small momentum regime of QCD using their DSEs. It has been shown that the gluon propagator or ghost propagator is sin-

Received 20 December 2005, Revised 17 March 2006
*Supported by National Natural Science Foundation of China (90103018, 90303006) and Jiangsu Province "333 Project" Fund
1) E-mail: jlping@njnu.edu.cn

gular in the infrared limit[10, 11]. The singularity will complicate the renormalization, which is necessary to extract the needed information. So far two renormalization prescriptions: the analytic continuation approach[12] and the subtraction approach[3], were used in the analysis of the infrared behavior of gluon and ghost propagators. Different results are obtained in different work. The present work is to compare the two different renormalization approaches in the infrared regime for the same DSEs with same approximations and to see whether the two approaches give us same results or not.

2 The DSEs for gluon and ghost propagators

The derivation of DSEs for ghost and gluon propagators has been given in Ref. [11]. Parameterizing the ghost propagator $D_{\rm G}$ and the gluon propagator $D_{\mu\nu}$ by their respective renormalization functions G and Z,

$$\begin{aligned} D_{\rm G}(k) &= -\frac{G(k^2)}{k^2}, \\ D_{\mu\nu}(k) &= \left(\delta_{\mu\nu}-\frac{k_\mu k_\nu}{k^2}\right)\frac{Z(k^2)}{k^2}, \end{aligned} \tag{1}$$

in the Landau gauge, with the bare three-gluon and gluon-ghost vertices, the DSEs for the ghost and gluon propagators lead to

$$G^{-1}(k^2)=\tilde{Z}_3-\frac{3g^2}{8\pi^3}\int_0^{\Lambda^2}{\rm d}q^2q^2G(q^2)\int_0^{\pi}{\rm d}\theta\frac{\sin^4\theta}{p^4}Z(p^2), \tag{2}$$

$$\begin{aligned} Z^{-1}(k^2) \;=\; & Z_3+\frac{g^2}{8\pi^3}\int_0^{\Lambda^2}\frac{{\rm d}q^2}{k^2}G(q^2)\int_0^{\pi}{\rm d}\theta\sin^2\theta \\ & M(k^2,q^2,p^2)G(p^2)+ \\ & \frac{g^2}{8\pi^3}Z_1\int_0^{\Lambda^2}\frac{{\rm d}q^2}{k^2}Z(q^2)\int_0^{\pi}{\rm d}\theta\sin^2\theta \\ & Q(k^2,q^2,p^2)Z(p^2), \end{aligned} \tag{3}$$

with $p^2=k^2+q^2-2pq\cos\theta$ and Λ^2 the ultraviolet cutoff. The kernels are

$$M(k^2,q^2,p^2)=\frac{1}{p^2}\left(\frac{k^2+q^2}{2}-\frac{q^4}{k^2}\right)+\frac{1}{2}+\frac{2q^2}{k^2}-\frac{p^2}{k^2},$$

$$\begin{aligned} Q(k^2,q^2,p^2) \;=\; & \left(\frac{k^6}{4q^2}+2k^4-\frac{15q^2k^2}{4}+\frac{q^4}{2}+\frac{q^6}{k^2}\right)\frac{1}{p^4}+ \\ & \left(\frac{2k^4}{q^2}-\frac{19k^2}{2}-\frac{13q^2}{2}+\frac{8q^4}{k^2}\right)\frac{1}{p^2}- \\ & \left(\frac{15k^2}{4q^2}+\frac{13}{2}+\frac{18q^2}{k^2}\right)+ \\ & \left(\frac{1}{2q^2}+\frac{8}{k^2}\right)p^2+\frac{p^4}{k^2q^2}. \end{aligned} \tag{4}$$

In the above equations, k, p and q denote the momenta of the propagators.

Refs. [11—13] have already revealed that in the infrared region the gluon renormalization function is infrared vanishing while the ghost renormalization function is infrared singular. For the infrared properties of the gluon and ghost propagators, it has been shown that the gluon propagator vanishes for the small momenta while the ghost propagator is infrared enhanced. Here we just do the infrared analysis, so the second term in Eq. (3) can be ignored. The equations to be studied become:

$$G^{-1}(k^2)=\tilde{Z}_3-\frac{3g^2}{8\pi^3}\int_0^{\Lambda^2}{\rm d}q^2q^2G(q^2)\int_0^{\pi}{\rm d}\theta\frac{\sin^4\theta}{p^4}Z(p^2), \tag{5}$$

$$\begin{aligned} Z^{-1}(k^2) \;=\; & Z_3+\frac{g^2}{8\pi^3}\int_0^{\Lambda^2}\frac{{\rm d}q^2}{k^2}G(q^2)\int_0^{\pi}{\rm d}\theta\sin^2\theta\times \\ & M(k^2,q^2,p^2)G(p^2). \end{aligned} \tag{6}$$

In the infrared regime, it was assumed that the ghost and gluon renormalization functions obeyed the power law[11, 13]:

$$Z(x) \;=\; Ax^{2\kappa}, \tag{7}$$

$$G(x) \;=\; Bx^{-\kappa}. \tag{8}$$

With these simplifications, Eqs. (5) and (6) reduce to (let $x=k^2, y=q^2, z=p^2=x+y-2\sqrt{xy}\cos\theta$)

$$\frac{x^\kappa}{B}=\tilde{Z}_3-\frac{6\lambda AB}{\pi}\int_0^{\Lambda^2}\frac{{\rm d}y}{y^{\kappa-1}}\int_0^{\pi}\frac{{\rm d}\theta\sin^4\theta}{z^{2-2\kappa}}, \tag{9}$$

$$\frac{x^{-2\kappa}}{A}=Z_3+\frac{2\lambda B^2}{\pi}\int_0^{\Lambda^2}\frac{{\rm d}y}{xy^\kappa}\int_0^{\pi}\frac{{\rm d}\theta\sin^2\theta}{z^{-\kappa}}M(x,y,z). \tag{10}$$

In Ref. [13], a further simplification, the y-max approximation, was introduced. In the y-max approximation, the κ was obtained as:

$$\kappa\approx 0.77. \tag{11}$$

And the running coupling, which is given by

$$\alpha(x)=4\pi\lambda Z(x)G^2(x), \tag{12}$$

has a non-trivial infrared fixed point

$$\alpha(0)\approx 11.4702. \tag{13}$$

Generally, the integrals in Eqs. (9) and (10) are divergent because of the singularity at $y=0$. The renormalization procedure should be employed to evaluate the integrals.

3 Two renormalization approaches

3.1 The analytic continuation approach

In Ref. [12], the analytic continuation approach was developed. The integral in Eq. (9) is convergent if Re $\kappa<0$, whereas a subtraction is necessary if $0<\kappa<1$. By identifying $\tilde{Z}_3$ with this subtraction constant, one ensures that $G(x)$ is defined by analytic continuation in κ beyond Re $\kappa=0$. This continuation is made explicit in terms of the generalized hypergeometric function.

By using the generalized hypergeometric function, the Eq. (9) can be evaluated and the result is shown below

$$\frac{1}{\lambda AB^2}=-\frac{9}{4}\Big[\frac{1}{2-\kappa}{}_3F_2(-2\kappa+2,-2\kappa,2-\kappa;3,3-\kappa;1)-\frac{1}{\kappa}{}_3F_2(-2\kappa+2,-2\kappa,-\kappa;3,1-\kappa;1)\Big]. \tag{14}$$

Similarly, Eq. (10) becomes

$$\begin{aligned}\frac{1}{\lambda AB^2}=\;&\frac{1}{2(1-\kappa)}{}_3F_2(\kappa+1,\kappa,1-\kappa;2,2-\kappa;1)+\frac{1}{2(2-\kappa)}{}_3F_2(\kappa+1,\kappa,2-\kappa;2,3-\kappa;1)-\frac{1}{1-\kappa}{}_3F_2(\kappa-1,\kappa-2,1-\kappa;2,2-\kappa;1)+\\&\frac{1}{2\kappa-2}{}_3F_2(\kappa-1,\kappa-2,2\kappa-2;2,2\kappa-1;1)+\frac{1}{2(2\kappa-1)}{}_3F_2(\kappa+1,\kappa,2\kappa-1;2,2\kappa;1)-\frac{1}{2\kappa-2}{}_3F_2(\kappa+1,\kappa,2\kappa-2;2,2\kappa-1;1)+\\&\frac{1}{2(1-\kappa)}{}_3F_2(\kappa,\kappa-1,1-\kappa;2,2-\kappa;1)+\frac{2}{2-\kappa}{}_3F_2(\kappa,\kappa-1,2-\kappa;2,3-\kappa;1)+\\&\frac{1}{2(2\kappa-1)}{}_3F_2(\kappa,\kappa-1,2\kappa-1;2,2\kappa;1)+\frac{1}{\kappa-1}{}_3F_2(\kappa,\kappa-1,2\kappa-2;2,2\kappa-1;1)-\frac{1}{3-\kappa}{}_3F_2(\kappa+1,\kappa,3-\kappa;2,4-\kappa;1)+\\&\frac{1}{4\kappa}{}_3F_2(\kappa+1,\kappa,2\kappa;2,2\kappa+1;1).\end{aligned} \tag{15}$$

Then the result of $\kappa\to 1$ and $\alpha(0)\approx 4.19$ is obtained. The behavior of the ghost and gluon propagators in the infrared regime is the same as that in y-max approximation mentioned above: the gluon renormalization function is infrared vanishing while the ghost renormalization function is infrared singular. The running coupling has an infrared fixed point. But the values of κ and $\alpha(0)$ are different from y-max approximation. So although y-max approximation is a good approximation for the ultraviolet analysis, it is not a good one for the infrared analysis.

Recently, a lot of work has been done in this subject and different results have been obtained in different work. Within the framework of the bare three-gluon and gluon-ghost vertices, Refs. [14—17] did the infrared renormalization using the analytic continuation approach with the help of Γ-functions. In their work, the contraction was performed using an arbitrary ξ-parameter tensor, and the infrared analysis yielded the bulk of solutions between κ=0.5 and κ=0.6 for different ξ when using a non-Brown-Pennington tensor[18]. For κ=0.595, the infrared fixed point is $\alpha(0)$=2.97. In Refs. [19,20], considering the multiplicative renormalization, a two-loop truncation of the ghost-gluon DSEs was performed, and with different groups of parameters, they obtained the results between κ=0.17 and κ=0.53. For κ=0.5, the infrared fixed point is $\alpha(0)$=5.24. The infrared behavior of the gluon and ghost propagators in the work mentioned above is consistent, although the values of $\alpha(0)$ and κ are different.

3.2 The subtraction approach

In this approach, the integration region $\int_0^{\Lambda^2}$ in Eq. (9) is separated into two parts: $\int_0^x$ and $\int_x^{\Lambda^2}$. For the integration over $\int_0^x$, we change the integral vari-

able:

$$y=xt,\quad \mathrm{d}y=x\mathrm{d}t,$$
$$z=x+y-2\sqrt{xy}\cos\theta=x(1+t-2\sqrt{t}\cos\theta),\quad (16)$$

and for the integration over $\int_x^{\Lambda^2}$,

$$y=\frac{x}{t},\quad \mathrm{d}y=-\frac{x\mathrm{d}t}{t^2},$$
$$z=x+y-2\sqrt{xy}\cos\theta=\frac{x}{t}(1+t-2\sqrt{t}\cos\theta).\quad (17)$$

Inserting Eqs. (16) and (17) into Eq. (9), we obtain:

$$\frac{x^\kappa}{B} = \tilde{Z}_3-\frac{6\lambda ABx^\kappa}{\pi} \left\{\int_0^1\frac{\mathrm{d}t}{t^{\kappa-1}}\int_0^\pi\frac{\mathrm{d}\theta\sin^4\theta}{(1+t-2\sqrt{t}\cos\theta)^{2-2\kappa}}+ \int_{x/\Lambda^2}^1\frac{\mathrm{d}t}{t^{1+\kappa}}\int_0^\pi\frac{\mathrm{d}\theta\sin^4\theta}{(1+t-2\sqrt{t}\cos\theta)^{2-2\kappa}}\right\}. \quad (18)$$

The renormalization constant $\tilde{Z}_3$ can be eliminated by subtracting the above equation at $x=s$, then we get

$$\frac{1}{\lambda AB^2}=\tilde{A}(\kappa)+\frac{x^\kappa\tilde{B}_1(\kappa,x)-s^\kappa\tilde{B}_2(\kappa,s)}{x^\kappa-s^\kappa} \quad (19)$$

where

$$\tilde{A}(\kappa)=-\frac{6}{\pi}\int_0^1\frac{\mathrm{d}t}{t^{\kappa-1}}\int_0^\pi\frac{\mathrm{d}\theta\sin^4\theta}{(1+t-2\sqrt{t}\cos\theta)^{2-2\kappa}},$$
$$\tilde{B}_1(\kappa,x)=-\frac{6}{\pi}\int_{x/\Lambda^2}^1\frac{\mathrm{d}t}{t^{1+\kappa}}\int_0^\pi\frac{\mathrm{d}\theta\sin^4\theta}{(1+t-2\sqrt{t}\cos\theta)^{2-2\kappa}},\quad (20)$$
$$\tilde{B}_2(\kappa,s)=-\frac{6}{\pi}\int_{s/\Lambda^2}^1\frac{\mathrm{d}t}{t^{1+\kappa}}\int_0^\pi\frac{\mathrm{d}\theta\sin^4\theta}{(1+t-2\sqrt{t}\cos\theta)^{2-2\kappa}}.$$

The same procedure is applied to Eq. (10), the result is:

$$\frac{1}{\lambda AB^2}=C(\kappa)+\frac{x^{-2\kappa}D_1(\kappa,x)-s^{-2\kappa}D_2(\kappa,s)}{x^{-2\kappa}-s^{-2\kappa}},\quad (21)$$

where

$$C(\kappa) = \frac{2}{\pi}\int_0^1\frac{\mathrm{d}t}{t^\kappa}\int_0^\pi\frac{\mathrm{d}\theta\sin^2\theta}{(1+t-2\sqrt{t}\cos\theta)^\kappa}\times \frac{t-4t\cos^2\theta+3\sqrt{t}\cos\theta}{1+t-2\sqrt{t}\cos\theta},$$
$$D_1(\kappa,x) = \frac{2}{\pi}\int_{x/\Lambda^2}^1\frac{\mathrm{d}t}{t^{2-2\kappa}}\int_0^\pi\frac{\mathrm{d}\theta\sin^2\theta}{(1+t-2\sqrt{t}\cos\theta)^\kappa}\times \frac{1-4\cos^2\theta+3\sqrt{t}\cos\theta}{1+t-2\sqrt{t}\cos\theta},\quad (22)$$
$$D_2(\kappa,s) = \frac{2}{\pi}\int_{s/\Lambda^2}^1\frac{\mathrm{d}t}{t^{2-2\kappa}}\int_0^\pi\frac{\mathrm{d}\theta\sin^2\theta}{(1+t-2\sqrt{t}\cos\theta)^\kappa}\times \frac{1-4\cos^2\theta+3\sqrt{t}\cos\theta}{1+t-2\sqrt{t}\cos\theta}.$$

From Eqs. (19) and (21), we obtain

$$C(\kappa)+\frac{x^{-2\kappa}D_1(\kappa,x)-s^{-2\kappa}D_2(\kappa,s)}{x^{-2\kappa}-s^{-2\kappa}}= \tilde{A}(\kappa)+\frac{x^\kappa\tilde{B}_1(\kappa,x)-s^\kappa\tilde{B}_2(\kappa,s)}{x^\kappa-s^\kappa}.\quad (23)$$

The l.h.s of the above equation is corresponding to the gluon propagator, while the r.h.s is corresponding to the ghost propagator. In the subtraction approach here, we do both the radial and angular integrations numerically. Choosing different sets of x and s, we obtain the results, which are shown in Fig.1.

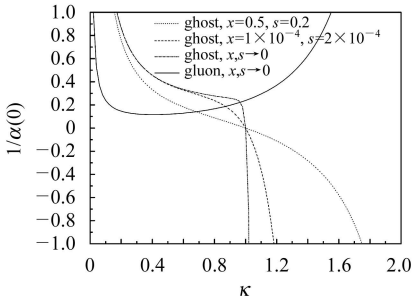

Fig. 1. The numerical result of κ.

From the numerical study, we find that the l.h.s of Eq. (23) (gluon part) is independent of the choices of x and s, while the r.h.s. of Eq. (23) (ghost part) depends on the choices of x and s. However, from Fig. 1, it is clear that when both x and s go to zero, $\kappa\to 1$ and $\alpha(0)\approx 4.19$ is obtained.

4 Summary

Taking bare three-point vertex functions in the truncated Dyson-Schwinger equations of gluon and ghost propagators, two renormalization approaches: analytic continuation approach and subtraction approach, are employed to investigate the infrared behavior of gluon and ghost propagators. The calculations show that the two renormalization approaches mentioned above give the same results in the infrared analysis. This is an important result, because we do not want to always take the bare vertices assumption. When the other information (i.e. the Slavnov-Taylor identities[11], transverse Ward-Takahashi identities[21,22]) can be used to determine the three-point vertices, the analytic continuation approach is not always possible in the infrared analysis,

while the subtraction approach can work. In addition, the subtraction approach works not only in the infrared regime but also in the whole momentum region.

References

1 Tandy P C. Prog. Part. Nucl. Phys., 1997, **39**: 117—199
2 Roberts C D, Williams A G. Prog. Part. Nucl. Phys., 1994, **33**: 477—575
3 Alkofer R, Smekal L V. Phys. Rept., 2001, **353**: 281—465
4 Miranski V A. Dynamical Symmetry Breaking in Quantum Field Theories. World Scientific, 1993
5 Munczek H J, Jain P. Phys. Rev., 1992, **D46**: 438—445
6 Cahill R T. Austr. J. Phys., 1989, **42**: 171—186
7 Ishii N, Bentz W, Yazaki K. Nucl. Phys., 1995, **A587**: 617—656
8 Hellstern G et al. Nucl. Phys., 1997, **A627**: 679—709
9 Roberts C D, Schmidt S M. Prog. Part. Nucl. Phys., 2000, **45**: S1—S103
10 Mandelstam S. Phys. Rev., 1979, **D20**: 3223—3238
11 Smekal L V, Hauck A, Alkofer R. Phys. Rev. Lett., 1997, **79**: 3591—3594
12 Atkinson D, Bloch J C R. Mod. Phys. Lett., 1998, **A13**: 1055—1062
13 Atkinson D, Bloch J C R. Phys. Rev., 1998, **D58**: 094036: 1—19
14 Fischer C S. 2003. hep-ph/0304233
15 Alkofer R, Detmold W, Fischer C S, Maris P. Phys. Rev., 2004, **D70**:014014: 1—26
16 Fischer C S, Alkofer R. Phys. Lett., 2002, **B536**: 177—184
17 Alkofer R, Fischer C S, Reinhardt H. Phys. Rev., 2003, **D68**:045003: 1—23
18 Brown N, Pennington M R. Phys. Rev., 1989, **D39**: 2723—2736
19 Bloch J C R. Phys. Rev., 2001, **D64**:116011: 1—11
20 Bloch J C R. Few-Body Systems, 2003, **33**: 111—152
21 HE H X, Khanna F C, Takahashi Y. Phys. Lett., 2000, **B480**: 222—228
22 HE H X. Commun. Theor. Phys., 2001, **35**: 32—35

红外区 Dyson-Schwinger 方程的两种重整化方案的比较*

石远美[1]　平加伦[1,2;1)]　何汉新[3]

1 (南京师范大学物理系和理论物理研究所　南京　210097)
2 (山东大学物理与微电子学院　济南　250100)
3 (中国原子能科学研究院　北京　102413)

摘要　在胶子和鬼传播子所满足的耦合的 Dyson-Schwinger 方程中, 采用裸胶子–鬼顶点, 利用两种重整化方案: 解析延拓方法和减除方法, 得到了胶子和鬼传播子的红外行为. 计算表明两种重整化方案在红外区对胶子和鬼传播子得到一致的结果.

关键词　Dyson-Schwinger 方程　非微扰 QCD　红外行为　囚禁　重整化途径

2005 – 12 – 20 收稿,　2006 – 03 – 17 收修改稿
*国家自然科学基金(90103018, 90303006)和江苏省“333”工程基金资助

1) E-mail: jlping@njnu.edu.cn